

Remote Image Analysis for Mars Exploration Rover Mobility and Manipulation Operations

P. Chris Leger
Jet Propulsion Laboratory
Pasadena, CA, USA
Chris.Leger@jpl.nasa.gov

Robert G. Deen
Jet Propulsion Laboratory
Pasadena, CA, USA
Bob.Deen@jpl.nasa.gov

Robert G. Bonitz
Jet Propulsion Laboratory
Pasadena, CA, USA
Robert.G. Bonitz@jpl.nasa.gov

Abstract - *NASA's Mars Exploration Rovers are two six-wheeled, 175-kg robotic vehicles which have operated on Mars for over a year as of March 2005. The rovers are controlled by teams who must understand the rover's surroundings and develop command sequences on a daily basis. The tight tactical planning timeline and ever-changing environment call for tools that allow quick assessment of potential manipulator targets and traverse goals, since command sequences must be developed in a matter of hours after receipt of new data from the rovers. Reachability maps give a visual indication of which targets are reachable by each rover's manipulator, while slope and solar energy maps show the rover operator which terrain areas are safe and unsafe from different standpoints.*

Keywords: Image understanding, teleoperation, Mars, rovers, MER, *Spirit*, *Opportunity*.

1 Introduction

NASA's Mars Exploration Rovers mission operates *Spirit* and *Opportunity*, two 175kg, 1.6m-long robotic vehicles on Mars [1]. Due to the time delay between Earth and Mars (driven primarily by the speed of light, but also limited time, power, and line-of-sight for communications), direct teleoperation of the rovers is impossible. Instead, each rover is operated by a team of engineers at the Jet Propulsion Laboratory (JPL) who build command sequences to drive the rover and operate its manipulator. Teams at JPL and elsewhere create command sequences to drive the rover and operate its cameras and science payload. In this paper, we describe some of the image analysis tools that aid the rover planning teams in assessing terrain for driving and manipulation.

2 Rover and Operations Overview

Each rover is equipped with four pairs of stereoscopic cameras: steerable navigation cameras (NavCams) and narrow field-of-view color cameras (PanCams), and two sets of hazard avoidance cameras (HazCams) [2]. These stereoscopic cameras are used in the generation of image products described in this paper. Each rover also has a Microscopic Imager and the Descent Imager, attached each rover's landing vehicle, acquired images just before

touchdown. All cameras share the same electronic design and software, but have different optics reflecting differing operational requirements.

Both sets of HazCams are mounted roughly 50cm above the ground and have fisheye lenses, allowing them to image terrain directly in front of and behind the rover. In addition to detecting hazards for autonomous navigation, the front HazCams are used by the rover operators and science team to select targets for each rover's arm, called the Instrument Deployment Device (IDD)[3]. The NavCams and PanCams are mounted on a two degree-of-freedom mast roughly 1.6m above the ground, allowing them to image terrain and sky in any direction. The raised vantage point of the NavCams and PanCams allows them to see terrain that is not visible to the HazCams, and their narrower fields-of-view (45 degrees for the NavCams and 14 degrees for the PanCams) yield higher spatial resolution than the HazCam. For human interpretation of images, the NavCams have an effective maximum range of 20-50m depending on terrain, lighting conditions, and image compression rates. The PanCams have an effective range of up to 200m. For reconstruction of terrain geometry the respective maximum useful ranges are roughly 4m, 20m and 80m for the HazCams, NavCams, and PanCams, respectively.

In addition to acquiring images for human interpretation, the stereoscopic cameras are also used by on-board software [4]. The HazCams are used for autonomous obstacle detection and avoidance, while the NavCams are used for Visual Odometry, which measures the rover's movement in order to compensate for slip on steep slopes. The PanCams are periodically used to track the sun's motion to refine the rovers' attitude knowledge, correcting for drift in the on-board inertial measurement units.

While raw camera images can give the rover operators some understanding of the rover's environments, images alone are insufficient since the rovers are controlled via quantitative commands. Therefore, the stereo image pairs are processed to extract geometric measurements of the terrain, which can be interpreted in a number of ways according to the needs of the day's command sequence. The rest of this paper describes several image-derived products specialized for rover operations.

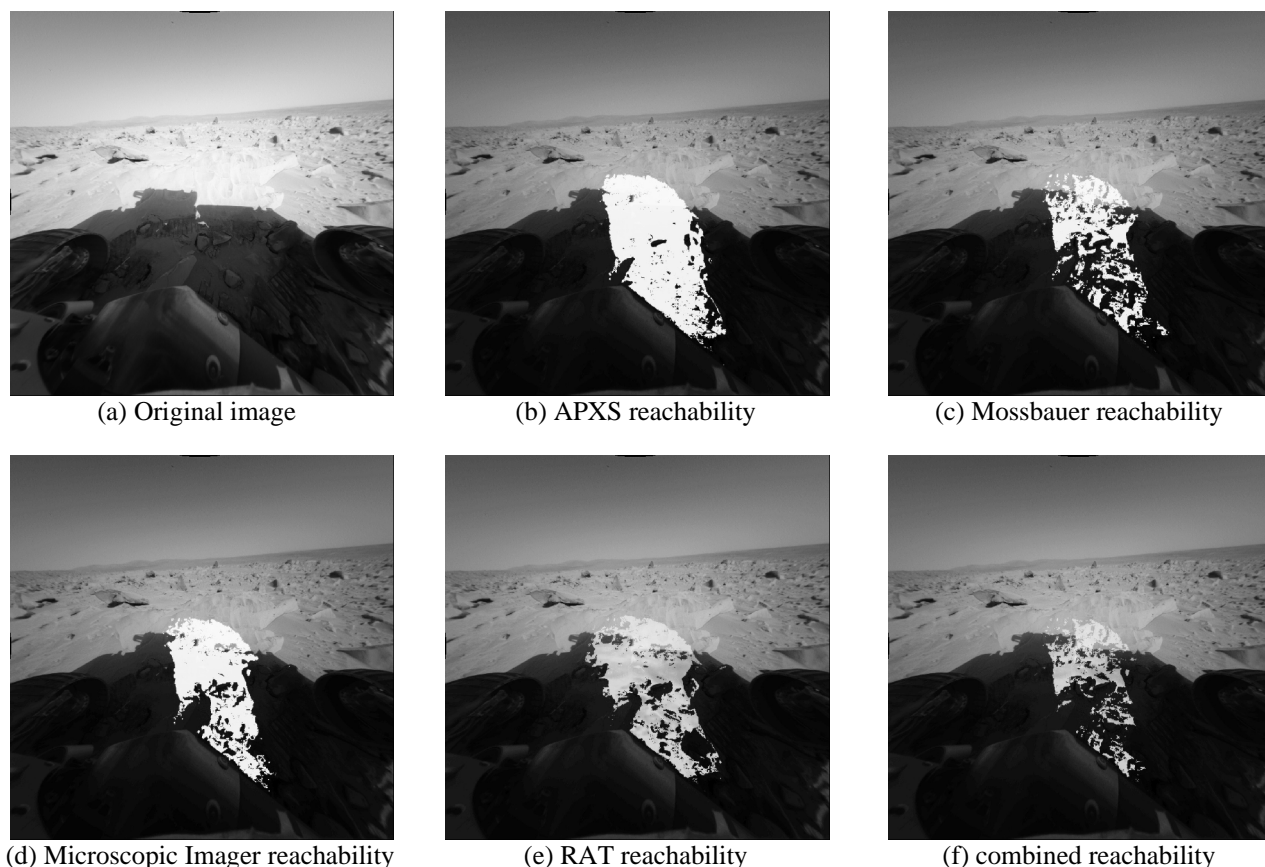


Figure 1: Front HazCam image of rock "Mazatzl" and derived reachability maps

3 Image Processing Architecture

Due to the tight tactical schedule for rover planning, image data must be processed quickly to enable the rover team to understand the rover's environment, select targets for science and navigation, and build command sequences. Image products are generated in a systematic, automated manner by a pipeline managed by the Multi-mission Image Processing Lab (MIPL) [5]. Up to 14 products are generated from each input image [6], ranging from radiometric correction to stereo correlation [7] to terrain generation [8] to reachability maps for manipulation and slope and solar energy maps for mobility assessment. Reachability and mobility maps are the focus of this paper.

The entire pipeline represents a data flow, with certain products not computable until others are ready. For example, the data flow to create a reachability map starts with the original 1024x1024 compressed image, which is radiometrically corrected, geometrically linearized, correlated with its stereo partner, and then triangulated to XYZ. The XYZ coordinates are used to compute surface normals, and both XYZ and surface normal products are used to compute reachability maps. The pipeline is triggered by the arrival of data from the spacecraft and, aside from special requests, the final products for each day's images are generally available in under an hour.

The pipeline products are used in a variety of ways. The Rover Sequencing and Visualization Program (RSVP, [9]) simulates rover driving and manipulation, using terrain meshes for visualization and for simulation of the rover's motion over terrain. High-quality panoramas composed of multiple NavCam and/or PanCam images can be viewed in a standalone tool, and image-based measurements of points and distances can be performed in RSVP or in the Science Activity Planner (SAP, [10]). Finally, a program called "marsviewer" can display any of the image-derived maps as color overlays over the original grayscale images, allowing properties such as slope or reachability by various arm-mounted instruments to be easily understood relative to the underlying terrain.

4 Image Maps for Manipulation

To meet planning deadlines throughout the day, the rover team must be able to quickly select feasible targets for manipulation. During early rover operations field tests with the FIDO rover [11], scientists selected targets in a HazCam image using SAP, then queried an external program to determine if a target was reachable by the manipulator. This proved inefficient, since the reachable areas are non-intuitive and are different for each of the arm-mounted instruments. To streamline operations, we began using *reachability maps* (Figure 1) which consist of

a color overlay indicating which instruments can reach the terrain at each pixel in an image. Reachability, rather than manipulability, is sufficient since target feasibility for MER is usually limited by kinematic configuration flips, joint limits, or self-collisions, rather than kinematic singularities. We therefore adopted reachability maps for MER and integrated their generation into the MIPL pipeline.

The generation of reachability maps begins with the XYZ (3D coordinate) and UVW (surface normal) images, which contain stereo-derived points and normals for each pixel in the original image. The surface normal for each point is computed by fitting a plane to all points within 2.5cm of the point being considered, then rejecting outliers and repeating the plane fit. This iteration is continued until either a minimum plane fit error is reached or until there are too few points for a reliable plane calculation, in which case the surface normal is marked as invalid. The 2.5cm distance threshold was chosen to be close to the radii of the contact surfaces of the arm-mounted instruments, though this is varied when computing surface normal maps for other purposes.

The next step in generating reachability maps consists of computing the IDD's inverse kinematics for the XYZ-UVW n-tuples at each image point. The inverse kinematics are computed separately for each of the four instruments, the Rock Abrasion Tool (RAT), Alpha Particle X-ray Spectrometer (APXS), Moesbauer Spectrometer, and Microscopic Imager. These instruments are mounted on a revolving turret at the end of the IDD, and differences in the instruments' position and orientation on the turret, as well as the differing tool lengths, lead to different kinematic solutions for each instrument. In addition, there can be multiple kinematic solutions (e.g. elbow-up or elbow-down) for each instrument. The multiple solutions are vetted against joint limit constraints and are checked for self-collisions using a geometric model of the arm. If a kinematic solution meeting the joint-limit and self-collision constraints remains, then the point is considered to be reachable by a given instrument. The multiple reachability values are combined into a multi-layered map which is overlaid on the original image to indicate which parts of the terrain are reachable. The user interface allows the overlay for each instrument to be toggled and combined in a logical AND, so that targets reachable for any subset of the instruments may be easily visualized.

The Rock Abrasion Tool has additional operational constraints compared to the other instruments. The RAT has two contact sensors which must be engaged before any other part of the RAT touches the surface. The contact sensors protrude roughly 1cm beyond the rest of the instrument, so that a surface may have protrusions up to 1cm in height and still be safe for RAT operations. RAT *roughness map* overlays provide immediate visual indication of which areas of a rock are sufficiently smooth to allow safe RAT operations. Like reachability maps, the roughness maps take XYZ and UVW images as input and iterate over all pixels. The computation at each pixel consists of locating the highest points along the direction of

the surface normal over an area the size of the RAT head, and finding the lowest points (also along the normal) in an outer annulus corresponding to the possible contact areas of the RAT's contact sensors. The difference between these two values is the roughness, in meters, of the surface. This measurement captures the geometric safety requirements of the RAT, namely that the highest parts of the target must be within 1cm of any possible position of the RAT contact sensors. In practice, the RAT roughness maps are not definitive, as they are quite sensitive to noise. Correlation is sensitive to image compression artefacts, and surface normal calculations are sensitive to correlation errors. Small changes in surface normals lead to a large changes in the distance-to-plane calculations used for roughness maps. To mitigate, low image compression rates are used when acquiring images for RAT targeting.

Another operational constraint for the RAT is the availability of sufficient preload force to prevent the RAT from slipping during brushing or grinding operations. The IDD applies a preload force after the RAT is in contact with the target by commanding further motion and relying on internal compliance to act as a spring. The maximum safe preload depends heavily on the position and orientation of the target. The rover's on-board software uses a stiffness model of the IDD to compute joint-space increments which, when commanded, result in the application of the desired preload. The IDD actuators are strong enough to cause damage to the arm in certain configurations, so the software also performs structural limit checks to safeguard the arm during preloading. This structural limit check is also run on the ground to create *preload maps* which show the maximum safe preload at each pixel in an image. Since preload depends on the location, surface normal, and kinematic solution at each pixel, preloads can be computed at the same time as reachability maps. Once a kinematic solution is computed for a pixel, the software computes preload commands in 10N increments and tests them for structural safety. The maximum safe preload is assigned to the corresponding pixel in the preload map.

The reachability, roughness, and preload maps increase the efficiency of the rover teams by giving an immediate first-order assessment of the feasibility of placing each instrument on all possible targets. Scientists first identify the regions or features of interest in a HazCam image, then select a number of candidate targets that appear feasible on the basis of the various maps and according to which instruments will be used. The rover planners can then assess target feasibility on a more detailed basis, accounting for other factors such as collisions with terrain, safety of the complete IDD trajectory, and presence of kinematic singularities near the targets. Surface normals or target positions must sometimes be manually "tweaked" to avoid singularities or joint limits and make the command sequence robust to uncertainty in the actual contact location of each instrument placement.

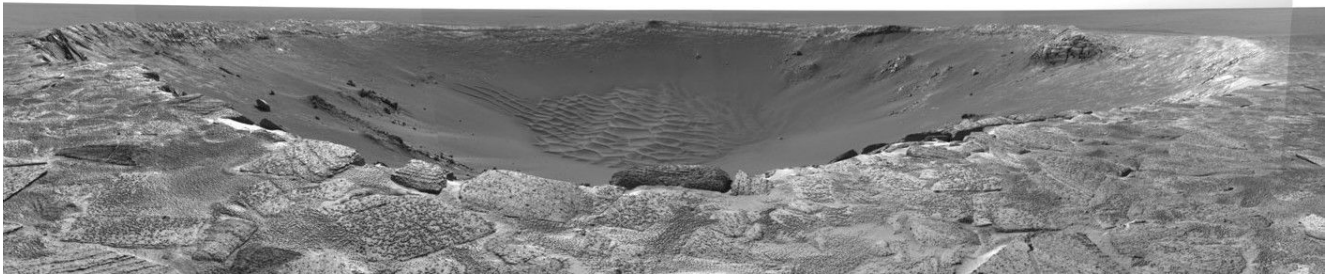


Figure 2: Endurance Crater, roughly 150m in diameter.

5 Maps for Rover Mobility

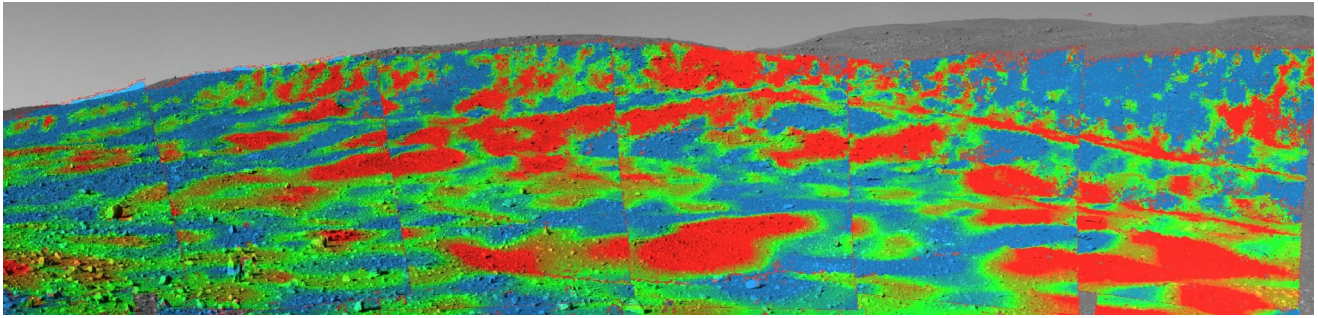
Planning a rover traverse involves quickly assessing many terrain properties and developing a command sequence that strikes a balance between vehicle safety and traverse efficiency. Rover operators have a number of on-board drive types at their disposal, including directed ("blind") drives, guarded drives in which the rover can image terrain and veto a predetermined motion, and AutoNav drives allowing the rover full autonomy. The rovers can also use image-based odometry ("visual odometry") to accurately measure the rover's position while driving in high-slip environments [4]. In an ideal world, the rovers would use visual odometry and hazard avoidance at all times, but this is impractical due to the slow processing speed of the rover's 20MHz CPU. Thus, blind drives are preferred when a hazard-free path can be seen in images, within the limits of the rover's positional accuracy. On level ground, the rover slips very little and the combination of inertial measurements and wheel odometry enables precise blind drives. In this case, the main hazards are rocks and negative obstacles such as ditches and craters. However, both rovers have spent most of their missions on sloped terrain, which present different hazards. A very steep slope or a moderate slope combined with rocks or significant sinkage can cause the rover to tip over, a certain mission-ender. Moderate slopes can cause high slip depending on the underlying material, and loose material on low slopes (10-13 degrees) can cause the wheels to sink and can block direct uphill progress.

Both *Spirit* and *Opportunity* encountered moderate slopes early in their missions, but slopes did not become the forcing function for mobility until *Opportunity* reached Endurance Crater (figure 2). Extensive outcrops of layered bedrock offered irresistible targets to the science team, and the engineering team had to assess whether *Opportunity* could safely enter the crater and, more importantly, get back out. The two primary considerations were terrain composition (sand or bedrock) and slope. The presence of some areas of bedrock were obvious from an initial NavCam survey, but slope assessment required a PanCam survey owing to the crater's 150m diameter.

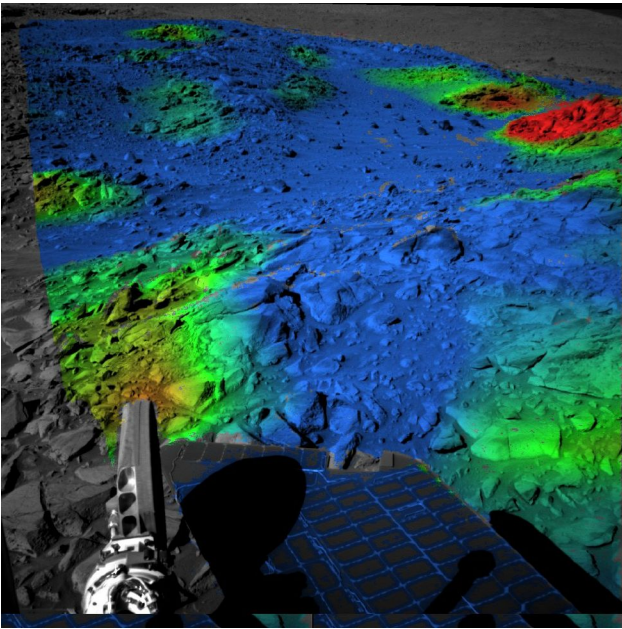
To create a high-level view of the crater's slopes, the MIPL team modified the surface normal portion of the image processing pipeline to compute a plane fit over rover-sized (1.6m diameter) patches, rather than instrument-sized (5cm diameter) patches. This required very large (several hundred pixel) window sizes, so the

computational efficiency was increased via adaptive sampling to adjust the sampling frequency within the window based on the range to the central pixel. After computing the surface normal, the slope was computed from the normal at each pixel, resulting in a slope map. Slope map generation was folded into the image processing pipeline so that new maps were available on a tactical basis. The team completed a PanCam slope survey of Endurance and conducted engineering tests with a duplicate rover at JPL, then identified an entry point with slopes of 15-20 degrees. *Opportunity* spent the next few months exploring Endurance and eventually climbed back to the plains.

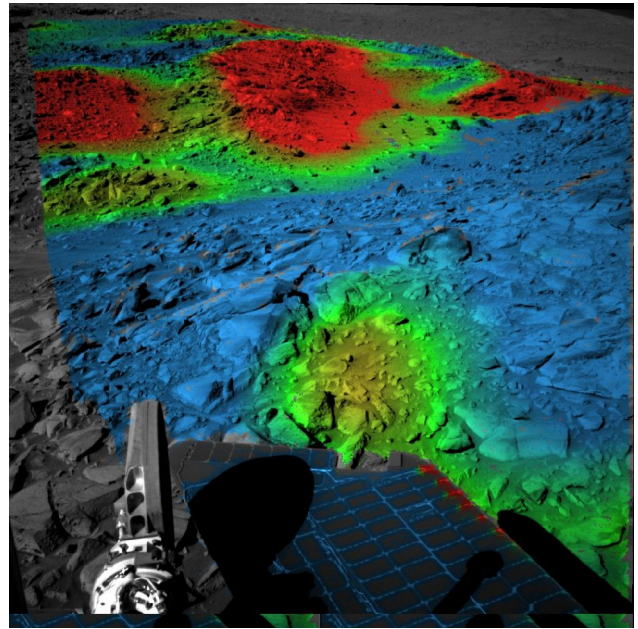
After crossing the plains to reach the Columbia Hills, *Spirit* also began driving on steep slopes. While the slopes were usually not as steep as those in Endurance Crater, the rugged and undulating nature of the terrain posed a different threat. With winter approaching at *Spirit's* southern-hemisphere landing site, available solar power depended heavily on whether the rover and its horizontally-mounted solar panels tilted to the North or South. If left on a south-facing slope for too long, *Spirit* would gradually deplete its batteries due to low solar energy input and would eventually be lost. Even on non-lethal slopes, *Spirit's* day-to-day capabilities were drastically impacted by northerly tilt. To ensure *Spirit's* safety and maximize solar input, we developed *solar energy maps* to assess the available solar energy at each point in the terrain. The *solar goodness* metric was defined as the dot product between the local surface normal and the vector pointing toward the sun at noon. This was a useful but not highly-accurate predictor of solar energy, since the actual energy also depended on details of the local terrain (e.g. which wheels were propped up on rocks), dust accumulation on the panels, large dust storms which attenuated the sun, and how much of the solar array was shadowed by the rover's mast and antenna. Still, the maps were an essential tool in safeguarding the rover. Our drive destinations were required to have a minimum solar goodness, since *Spirit* often spent several days in one place, and our routes were required to avoid areas of bad solar energy input so that if the drive triggered a fault and halted early, the rover would have sufficient energy to continue the next day.



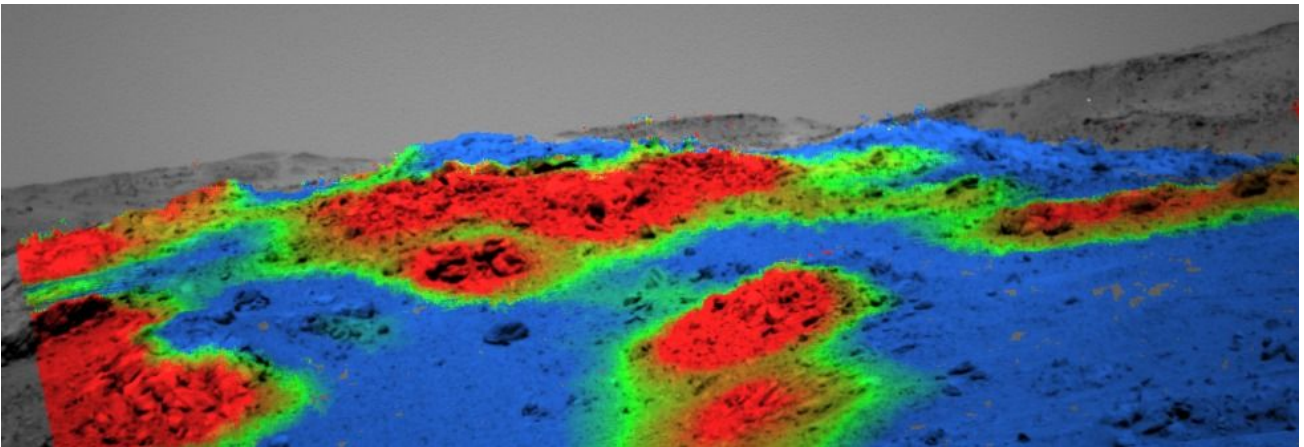
(a) PanCam solar energy mosaic of the West Spur. Discontinuities are image boundaries.



(b) NavCam slope map on the West Spur



(c) NavCam solar energy map on the West Spur



(d) NavCam slope map of Larry's Lookout on Cumberland Ridge, with slopes ranging up to 25 degrees.

Figure 3: Slope and Solar Energy Maps. In (a) and (c), blue indicates favorable tilt for solar energy, green is marginal, and red indicates unacceptable tilt. In (b) and (d), blue areas have low overall slope, green areas are moderate, and red areas have high slope.

Like slope maps, solar energy maps are viewed as color overlays on the original image. Figure 3 shows several slope and solar energy maps used for drive planning with *Spirit*. Figure 3(a) shows a solar energy map for on a PanCam mosaic of the West Spur. Since the slope faces West, solar energy was largely unacceptable and *Spirit* drove to the north before climbing onto the spur. Figures 3(b) and 3(c) show slope and solar energy maps, respectively, for a NavCam image acquired while on the West Spur. *Spirit* traveled up the green chute at the right of figure 3(c) in order to reach a high point on the West Spur and allow imaging of Husband Hill, the highest peak in the Columbia Hills. Figure 3(d) shows a NavCam slope map of Larry's Lookout. *Spirit* encountered 15 to 50% slip while driving to the ridge crest via the blue chute at right.

6 Conclusions

Planetary rover operation on a tight daily schedule requires a means of rapidly assessing the feasibility of manipulator targets and traverse paths. Images can give a rover operator some sense of the terrain and 3D terrain models are useful for simulation, but color overlays can quickly impart quantitative knowledge of the image scene to the operator. Using slope and solar energy maps, rover operators can quickly perform initial route finding by ruling out high-slope or low-energy areas. Reachability maps give rover operators and science team members the ability to intuitively see which parts of the immediate terrain are reachable by the manipulator, saving time on a tactical basis by eliminating trial-and-error target selection.

MIPL's automated image processing pipeline was essential in the timely delivery of image products on a daily basis--crucial on days when the relative phasing of Earth and Mars meant that a complex plan must be developed, sequenced, and uplinked within only 4 to 5 hours, compared to multiple days or weeks for many remote-sensing applications. The existing image processing infrastructure allowed rapid deployment of new tools, sometimes in the same day as the request for a new product.

The utility of image overlays suggests future areas for interface development. Currently, the terrain meshes used in the 3D rover simulation and visualization system are texture-mapped with the intensity values from the original images. Texture maps using color overlays would add an additional modality of terrain understanding, and will likely be incorporated in future versions of the software.

7 Acknowledgements

The research described in this paper was carried out at the Jet Propulsion Laboratory, California Institute of Technology, under a contract with the National Aeronautics and Space Administration. Thanks to MIPL for rapid deployment of new tools and quick turnaround of image products. Reachability maps were first incorporated into SAP by Jeff Norris and others. Larry Soderblom was key in formulating solar energy maps.

8 References

- [1] S. W. Squyres, et al. "The *Spirit* Rover's Athena Science Investigation at Gusev Crater, Mars". *Science*, Vol. 305, No. 5685, 6 August 2004.
- [2] J. N. Maki, et al. "Mars Exploration Rover Engineering Cameras", *Journal of Geophysical Research*, Vol. 108, No. E12.
- [3] E. Baumgartner, R. Bonitz, J. Melko, L. Shiraishi and C. Leger. "The Mars Exploration Rover Instrument Positioning System." In the Proceedings of the 2005 IEEE Aerospace Conference, Big Sky, MT, March 2005.
- [4] S. Goldberg, M. Maimone, L. Matthies, "Stereo Vision and Rover Navigation Software for Planetary Exploration." In Proceedings of the 2002 IEEE Aerospace Conference.
- [5] D. Alexander, P. Zamani, B. Deen, "The MIPL Pipeline: Automated Generation of Image Products for Mars Exploration Rover Mission Tactical Operations." In Proceedings of the 2005 IEEE Conference on Systems, Man, and Cybernetics.
- [6] R.G. Deen, D.A. Alexander, J.N. Maki, "Mars Image Products: Science Goes Operational", Proceedings of the 8th International Conference on Space Operations (SpaceOps), Montreal, Canada, 2004.
- [7] R. Deen, "Seeing in Three Dimensions: Correlation and Triangulation of Mars Exploration Rover Stereo Imagery." In Proceedings of the 2005 IEEE Conference on Systems, Man, and Cybernetics.
- [8] J. Wright, A. Trebi-Ollennu, J. Morrison, "Terrain Modeling for In-situ Activity Planning and Rehearsal for the Mars Exploration Rovers." In Proceedings of the 2005 IEEE Conference on Systems, Man, and Cybernetics.
- [9] J. Norris, M. Powell, M. Vona, P. Backes, J. Wick. "Mars Exploration Rover Operations with the Science Activity Planner." In Proceedings of the IEEE Conference on Robotics and Automation, Barcelona, Spain, April 2005.
- [10] J. Yen, B. Cooper, F. Hartman, S. Maxwell, J. Wright, "Sequence Rehearsal and Validation on Surface Operations of the Mars Exploration Rovers." In Proceedings of SpaceOps 2004, Montreal, Canada, 2004.
- [11] P Backes, et al. "Sequence Planning for the FIDO Mars Rover Prototype." In Proceedings of the 2003 IEEE Aerospace Conference, Big Sky, MT.